ISSN 1063-7834, Physics of the Solid State, 2008, Vol. 50, No. 11, pp. 2175–2183. © Pleiades Publishing, Ltd., 2008.
Original Russian Text © V.D. Fokina, I.N. Flerov, M.S. Molokeev, E.I. Pogorel'tsev, E.V. Bogdanov, A.S. Krylov, A.F. Bovina, V.N. Voronov, N.M. Laptash, 2008, published in Fizika Tverdogo Tela, 2008, Vol. 50, No. 11, pp. 2084–2092.

LATTICE DYNAMICS AND PHASE TRANSITIONS

Heat Capacity, p–T Phase Diagram, and Structure of Rb_2KTiOF_5

V. D. Fokina[a, b], I. N. Flerov[a, b], M. S. Molokeev[a], E. I. Pogorel'tsev[b], E. V. Bogdanov[a], A. S. Krylov[a], A. F. Bovina[a], V. N. Voronov[a], and N. M. Laptash[c]

[a] *Kirensky Institute of Physics, Siberian Branch, Russian Academy of Sciences, Akademgorodok, Krasnoyarsk, 660036 Russia*
e-mail: fokina@iph.krasn.ru

[b] *Siberian Federal University, pr. Svobodnyĭ 59, Krasnoyarsk, 660074 Russia*

[c] *Institute of Chemistry, Far East Division, Russian Academy of Sciences, pr. Stoletiya Vladivostoka 159, Vladivostok, 690022 Russia*

Received March 24, 2008

Abstract—Elpasolite Rb_2KTiOF_5 (space group $Fm\bar{3}m$, $Z = 4$) was synthesized using a solid-phase reaction method. The temperature dependences of the heat capacity, the unit cell parameters, the structure, the permittivity, the response to an external pressure, and the Raman spectra were studied. A nonferroelectric phase transition was revealed at $T_0 = 215$ K; the transition is accompanied by a tetragonal distortion of the unit cell (space group $I4/m$, $Z = 10$) and a change in the entropy ($\Delta S_0 \approx R\ln 8$), which is anomalously large for perovskite-like oxyfluorides with atomic cations. The specific features of the mechanism of structure distortion are discussed in combination with the previous experimental data obtained for cryolite $(NH_4)_3TiOF_5$ and elpasolite Rb_2KGaF_6.

PACS numbers: 61.50.Ks, 65.40.Ba, 65.40.gd, 78.30.Hv, 81.30.Dz

DOI: 10.1134/S1063783408110280

1. INTRODUCTION

Interest in crystals with quasi-octahedral anions containing mixed ligands, in particular, oxygen and fluorine atoms, is due to many factors. First, oxyfluorides are closer to oxides in terms of chemical stability and exhibit physical properties characteristic of both oxides and fluorides. Second, by varying the ligand content in an anion, very diverse structural types of fluorine–oxygen compounds can be created. Third, the noncubic symmetry of the six-coordinated anion offers wide possibilities of developing primarily noncentrosymmetric materials and, on the other hand, owing to statistical disordering of ligands, crystalline structures with cubic symmetry exist undergoing various phase transitions.

In the 1980s, researchers fairly actively studied oxyfluorides with perovskite-like cubic structure of the elpasolite–cryolite type (space group $Fm\bar{3}m$, $Z = 4$) formed by octahedra MO_3F_3 (M = W, Mo), for which two variants of local symmetry are possible: the orthorhombic C_{2v} for the *cis* configuration of ligands and the trigonal C_{3v} for the *fac* configuration [1, 2]. It has been revealed that many crystals having the general chemical formula $A_2A'MO_3F_3$ (A, A' = K, Rb, Cs), as well as related oxides, can be in ferroelectric and ferroelastic states. The temperature at which the cubic phase of oxyfluorides becomes unstable varies within wide limits depending on the combination of univalent cations. If the A and A' cations differ significantly in size, as, for example, in the case of the combination Cs_2K, the $Fm\bar{3}m$ phase remains stable down to 10 K [3].

Fluorine–oxygen compounds with another type of the quasi-octahedron, in particular, $TiOF_5$, have been studied to a significantly lesser degree. Crystallochemical and structural analyses of the conditions of possible existence of oxyfluorides $A_2A'MO_xF_{6-x}$ (x = 1, 2, 3) showed that, at room temperature, elpasolites $A_2A'TiOF_5$ (A, A' = Li, Na, K, Rb, Cs) exhibit a cubic structure and cryolites A_3TiOF_5 exhibit a pseudotetragonal structure [4]. According to infrared spectroscopy of titanium-containing oxyfluorides, the $TiOF_5$ anion exhibits tetragonal symmetry C_{4v} [5].

Later [6], it was revealed that the low-symmetric structure of titanium cryolites (A = K, Rb, Cs) is transformed on heating to the cubic structure (space group $Fm\bar{3}m$) as a result of one or two structural transformations. In [6], the polarization-optical measurements showed the existence of the ferroelastic state of A_3TiOF_5 in distorted phases, and it was assumed that the transition from the cubic phase in these compounds is accompanied by the appearance of a spontaneous polarization, as it is the case in oxyfluorides $A_2A'MO_3F_3$

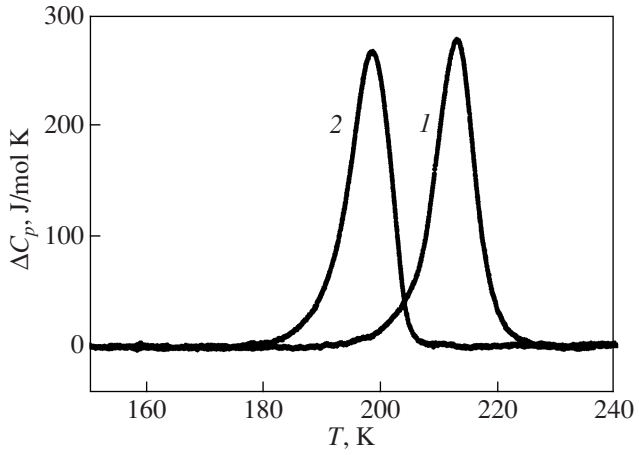

Fig. 1. Temperature dependence of the excess heat capacity of Rb_2KTiOF_5 measured by the DSM method upon (*1*) heating and (*2*) cooling.

[1]. On the other hand, it was established in [7] that the Na_3TiOF_5 crystal undergoes a ferroelastic phase transition $Fm\bar{3}m \rightleftharpoons P2_1/n$. It should be noted that the authors of [6, 7] indicated only the temperatures of the corresponding structural transformations and did not report any data on other thermodynamic parameters of the phase transitions. Thus, until recently, the fluorine–oxygen $A_2A'TiOF_5$ compounds remained poorly studied and many questions remained unanswered. Among them, the questions concerning (1) the type and mechanism of structural distortions in cryolites A_3TiOF_5, (2) the possible phase transitions in $A_2A'TiOF_5$ crystals with the elpasolite structure and the origin and mechanism of these phase transitions, and (3) the character of thermal atomic motion and the degree of disordering of the cubic and distorted phases.

Recently, on the one hand, the interest in studying oxyfluorides with atomic cations has revived at a new level [8–10] and, on the other hand, studies on the stability of the cubic phase of oxyfluorides containing the nonspherical ammonium cation in its structure have been performed [11–15]. In the former case [8–10], it has unambiguously been shown that the ferroelectric–ferroelastic phase in a number of $A_3MoO_3F_3$ crystals (A = Na, K, Tl) exhibits triclinic symmetry. In [11–15], it was shown that the simultaneous substitution of tetrahedral ammonium cations for spherical atomic cations in two nonequivalent crystallographic positions 8*c* and 4*b* (in some cases, only in 8*c*) results in the following effects. First, the stability temperature of the $Fm\bar{3}m$ phase decreases significantly and phase transitions occur mainly below room temperature [11–13, 15]. Second, at least in the tungsten-containing compounds, distorted phases are ferroelastic (space group $P2_1/n$) [3, 14]. Third, a significant disordering of the $Fm\bar{3}m$ structure is possible in both elpasolites–cryolites $A_2A'MO_3F_3$ and cryolites A_3TiOF_5. Fourth, according to calorimetric studies [15], in which the entropies of the phase transitions at atmosphere pressure (~Rln8) were determined, the degrees of disordering of the structures formed by octahedral $WO_3F_3^{3-}$ and $TiOF_5^{3-}$ anions are identical. At the same time, the DTA studies under pressure revealed a high-pressure phase on the pressure–temperature diagram of an $(NH_4)_3TiOF_5$ crystal and established that the change in the entropy due to successive phase transitions under pressure to this distorted phase is significantly larger (~Rln 24).

To answer some of the above questions concerning the oxyfluorides containing the $TiOF_5^{3-}$ anion in its structure, we studied in this work the heat capacity, the structure of the cubic and distorted phases, the unit cell parameters, the permittivity, the pressure–temperature phase diagram, and the Raman spectra of elpasolite Rb_2KTiOF_5.

2. SYNTHESIS AND CHARACTERIZATION OF SAMPLES AND SEARCH FOR PHASE TRANSITIONS

The compound Rb_2KTiOF_5 was synthesized using two solid-phase reaction methods. As the primary reagents taken in stoichiometric proportions, we used RbF, K_2TiF_6, and TiO_2 in one method and Rb_2CO_3, KF, and $(NH_4)_3TiOF_5$ in another method. In both the methods, the compound in the form of a highly dispersed powder was obtained by sintering at a temperature of 600°C; then, the material was placed into a platinum test tube and melted in a vertical gradient furnace at 960°C in an argon atmosphere and then it was crystallized at a rate of 0.9 mm/h.

The characterization of the fine-crystalline powders prepared by both the methods was performed using a DRON-2 x-ray powder diffractometer. It is established that, at room temperature, the compound is characterized by a cubic elpasolite structure with space group $Fm\bar{3}m$ (Z = 4). Both the samples exhibit identical Raman and infrared spectra.

In order to detect phase transitions, we first measured the heat capacity of Rb_2KTiOF_5 using a DSM-2M differential scanning microcalorimeter. The heat capacity was measured in the temperature range 130–280 K on heating and cooling at a rate of 8 K/min for several samples of the same crystallization and also for samples prepared by the different methods. The sample mass was varied from 0.10 to 0.25 g. Figure 1 shows the typical results of the DSM measurements on Rb_2KTiOF_5 in the form of the temperature dependence of the excess heat capacity obtained by subtracting the regular contribution from the measured total heat capacity. An anomaly of the Rb_2KTiOF_5 heat capacity is observed in the form of a sharp peak at a temperature T_0 = 214 ± 1 K. The significant thermal hysteresis

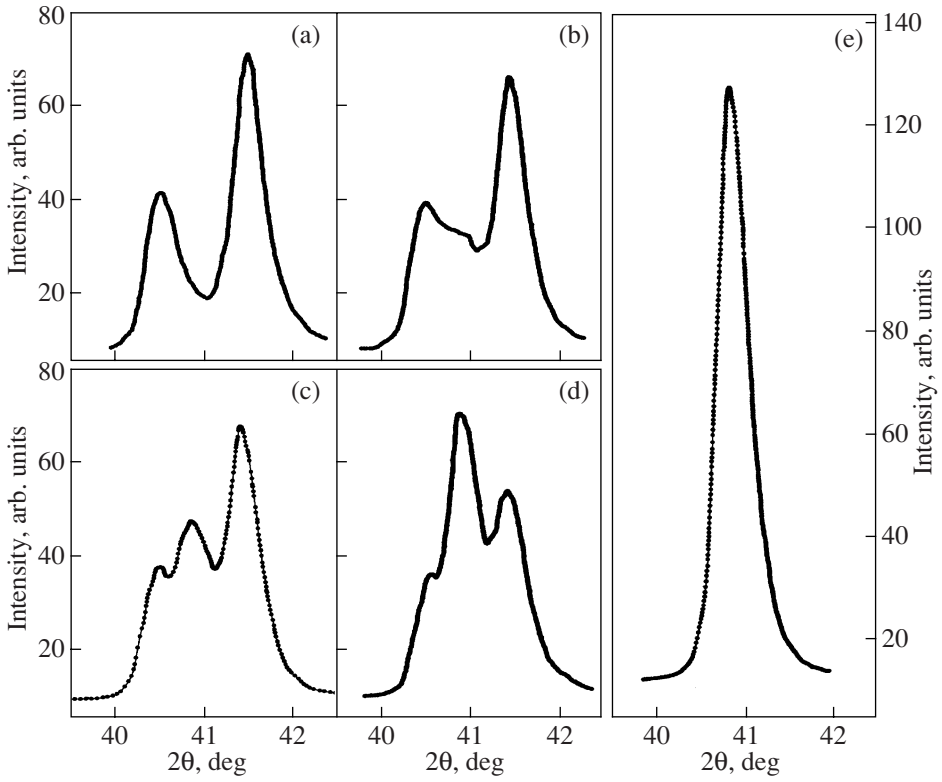

Fig. 2. Transformation of the (400) reflection at temperatures of (a) 193, (b) 208, (c) 213, (d) 218, and (e) 293 K.

($\delta T_0 \approx 15$ K) clearly indicates that the structural transformation is of first order. The transition enthalpy as determined by integrating the function $\Delta C_p(T)$ over the temperature range 190–225 K is $\Delta H_0 = 2300 \pm 400$ J/mol.

The structural phase transition in Rb_2KTiOF_5 is confirmed by the results of studying the powders on a DRON-2 x-ray diffractometer at room temperature and at $T < T_0$. The x-ray diffraction patterns of the distorted phase show broadened and split (h00) and (hk0) reflections. The variation of the (400) reflection with temperature is shown in Fig. 2. In the ~15-K-wide temperature range below T_0, this reflection is split into three reflections, of which only two reflections survive at lower temperatures.

At first glance, this phenomenon can be explained by the occurrence of two phase transitions (e.g., to an orthorhombic phase and then to a tetragonal one). It should be noted, however, that the position of the peak corresponding to the (400) reflection of the cubic phase remains unchanged over the range of its existence at $T < T_0$. At the same time, a strongly pronounced intensity redistribution is observed, as a result of which only two peaks are retained below ~205 K. Based on these facts, another interpretation of the transformation of the (400) reflection can also be proposed. In the ~12-K-wide temperature range below T_0, a cubic phase and a distorted (perhaps tetragonal) crystal structure coexist in Rb_2KTiOF_5, and the above intensity redistribution corresponds to a change in the amounts of the material in the different phases. In this case, there are no transition kinetics; namely, the x-ray diffraction pattern remains unchanged after 4 h of holding of the sample at the temperature corresponding to the two-phase state.

The temperature dependence of the crystal lattice parameters will be considered after the refinement of the distorted phase structure.

3. DIELECTRIC MEASUREMENTS

As mentioned above, the phase transitions occurring in cryolites A_3TiOF_5 (A = K, Rb, Cs) were previously assigned to ferroelectric transitions [6]. At the same time, studies of the oxyfluorides with the $MO_3F_3^{3-}$ anion show that the transitions are ferroelectric in both the cases $A = A'$ and $A \neq A'$ [16]. Therefore, in order to establish the character of the structural transformation in the elpasolite Rb_2KTiOF_5, we measured its permittivity as a function of temperature. Since we have no single-crystal samples, the measurements were carried out on ceramic samples in the shape of cylindrical pellets 8.04 mm in diameter and 2.27 mm in height prepared by the traditional technology, namely, by compaction and sequent burning at 650°C. Copper electrodes were deposited on a sample in a vacuum.

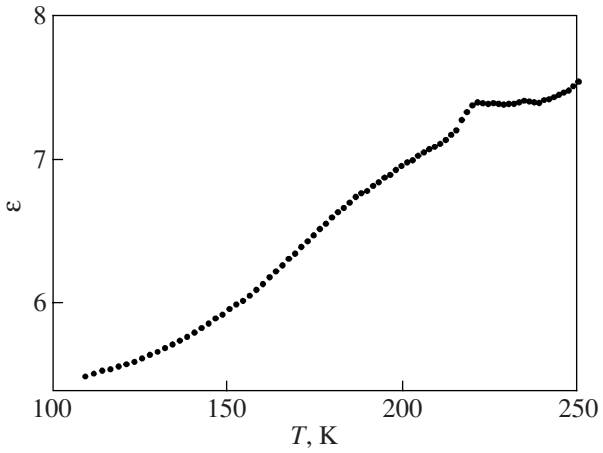

Fig. 3. Temperature dependence of the permittivity of Rb_2KTiOF_5.

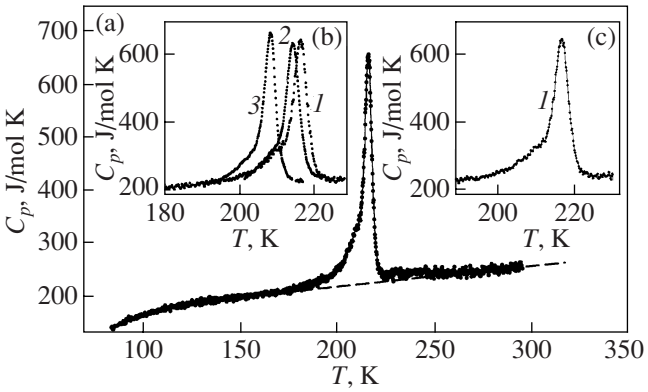

Fig. 4. Temperature dependences of the molar heat capacity of Rb_2KTiOF_5 (a) over a wide temperature range and (b, c) measured near T_0 (*1*, *2*) on heating at a rate of (*1*) 0.16 and (*2*) 0.06 K/min and (*3*) on cooling at a rate of 0.06 K/min.

The $\varepsilon(T)$ dependence was measured using an E7-20 immitance meter at a frequency of 1 kHz in the temperature range 110–260 K on heating at a rate of ~1 K/min. The results of measurements are presented in Fig. 3. The permittivity increases slowly from 5.5 to 7.0 in the range 110–205 K, and the rate of increase becomes somewhat higher with a further increase in temperature. At T = 215–217 K, i.e., near the phase transition temperature T_0 as measured in calorimetric and x-ray diffraction experiments, a smeared jump occurs. Above this temperature, the value of εremains practically constant up to 235 K, and then it increases with temperature.

4. HEAT CAPACITY AND HYDROSTATIC-PRESSURE RESPONSE

Detailed measurements of the Rb_2KTiOF_5 heat capacity were performed in the range 85–295 K using an adiabatic calorimeter. The powder sample under study with a mass of 0.91 g was packed into a copper container, which, in turn, was hermetically sealed in an indium envelope under helium atmosphere. Then, the entire system was placed into a furniture (an aluminum foil with a glued constantan-wire heater). To provide a good thermal contact between the indium envelope and the furniture, we used a vacuum lubricant with a mass of 9 mg, whose heat capacity was measured in [17]. The heat capacity was measured upon discrete heating in calorimetric steps of ~2.5 K and upon continuous heating at a rate dT/dt = 0.16–0.22 K/min.

The temperature dependence of the molar heat capacity of Rb_2KTiOF_5 is presented in Fig. 4a. The $C_p(T)$ curve exhibits a pronounced anomaly in the shape of an asymmetric peak with a maximum at a temperature $T_0 = 217.0 \pm 0.5$ K, which, in our opinion, is due to a phase transition. At $T < T_0$, near 208–210 K, a small shoulder-like anomaly is also observed (Fig. 4c).

Figure 4b presents the results of studying the immediate vicinity of the phase transition using the method of quasistatic thermograms, which were measured at an average rate of heating and cooling $|dT/dt| \approx$ 0.06 K/min. The shape of the heat capacity anomaly and the value of its maximum are practically independent of the sample heating rate, as can be seen from comparing curves *1* and *2* in Fig. 4b obtained at heating rates differing by a factor of about three. In a series of thermographic experiments, however, the transition temperature is found to be lower ($T_0 = 215.0 \pm 0.5$ K). In what follows, we assume that this value corresponds to conditions that are closest to equilibrium. In this case, the shoulder at $T < T_0$ is smeared over an even wider temperature range. A decrease of more than two orders of magnitude in the rate of temperature variation as compared to the DSM-2M experiments leads to significantly decreased hysteresis ($\delta T_0 = 6.1$ K).

It should be noted that the margin of error in determining T_0 is very large and practically independent of the temperature variation rate. The reason for this is that the excess heat capacity peak (whose position is used to determine the transition temperature) is fairly spread and its maximum is not clearly defined. This is reflected in the absence of a horizontal (or slightly inclined) thermogram segment corresponding to the absorption and release of the latent heat upon heating and cooling, respectively. It appears unusual, because the hysteresis of the transition temperature is large, as mentioned above.

In order to find the thermodynamic functions related to the phase transition, we subtracted from the total heat capacity of Rb_2KTiOF_5 the lattice contribution, which is determined by fitting the experimental data outside the range of existence of the anomaly by a polynomial (as shown by the dashed curve in Fig. 4a). The excess heat capacity ΔC_p exists over a significantly wider temperature range of the distorted phase ($T_0 - T$) ≈ 50 K

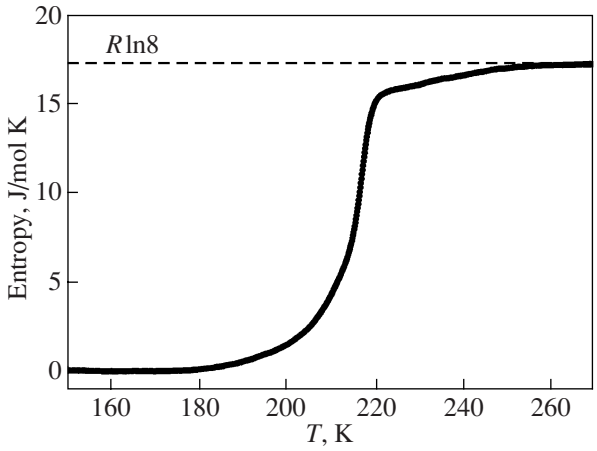

Fig. 5. Temperature dependence of the entropy during the phase transition in Rb_2KTiOF_5.

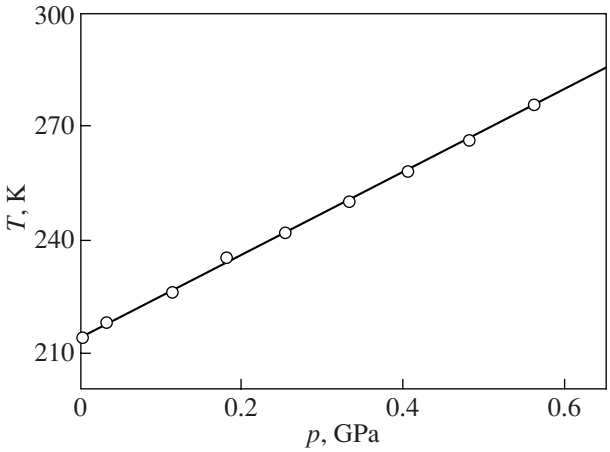

Fig. 6. p–T phase diagram of Rb_2KTiOF_5.

(Fig. 4a) than it follows from the DSM-2M measurements. Above T_0, it is observed up to 260 K.

As a result, the phase transition enthalpy as determined by integrating the $\Delta C_p(T)$ function over the temperature range 170–260 K is $\Delta H_0 = 3600 \pm 200$ J/mol, which is substantially higher than that found from the DSM experiments. By integrating the function $(\Delta C_p/T)(T)$, we studied the behavior of the entropy (Fig. 5), whose total change is $\Delta S_0 = 17.0 \pm 0.9$ J/mol K.

The pressure–temperature phase diagram was studied using the differential thermal analysis (DTA) technique that we used previously when studying a number of other oxyfluorides [11–13, 15]. A germanium–copper thermocouple (sensitive DTA element), together with a sample and a standard specimen attached to its junctions, was placed into a high-pressure cylinder–piston-type chamber filled with a mixture of pentane and transformer oil. The pressure in the chamber ranging from 0 to 0.6 GPa was produced and controlled using a pumping plant and a multiplier. The temperature and pressure were measured with an accuracy of ±0.3 K and $\pm 10^{-3}$ GPa, respectively. The experiments were performed under increasing and decreasing pressure, which allows us to study the reproducibility of the results obtained. The technique used permits one to measure the $T(p)$ dependence only upon heating of the high-pressure chamber with the sample. Because of this, thermal hysteresis was not studied.

Figure 6 shows the p–T phase diagram constructed using the measurement results. It follows from Fig. 6 that an increase in pressure favors the stabilization of the distorted phase; namely, the phase transition temperature increases. The phase boundary is described by the equation $T_0 = 214.3 + 109.6p - 1.4p^2$. Since the coefficient of p^2 is small, the boundary is an almost straight line, and it is characterized by a large pressure coefficient $dT_0/dp = 109.6$ K/GPa.

5. CRYSTAL STRUCTURE

The calorimetric studies of oxyfluoride Rb_2KTiOF_5 revealed that the phase transition in this compound is accompanied by a fairly large change in the entropy ($\Delta S = \ln 7.7$), which is characteristic of order–disorder transformations. To study the mechanism of structural distortions, we carried out a detailed x-ray diffraction study of the initial and distorted phases.

The x-ray diffraction patterns of a Rb_2KTiOF_5 polycrystalline sample were obtained at various temperatures using a SMART APEXII single-crystal diffractometer with a two-coordinate detector (MoK_α radiation). In this experiment, owing to the use of a two-coordinate detector and the possibility of rotating the sample holder, we excluded the influence of texture and size nonuniformities of powder grains. However, due to the large diameter of the collimator used in this technique, the peak half-width is significant in the powder experiment. As a result, we failed to detect the splitting of the (400) reflection of the $Fm\bar{3}m$ phase into three reflections observed with a DRON-2 diffractometer within the 15-K-wide range below T_0 (see Section 2). Immediately after the phase transition, this reflection is merely broadened. Only much below T_0 did we reliably detect its splitting into two peaks. The details of the structural studies will be reported in a future publication.

The scanned diffraction patterns obtained in this experiment are integrated, and the unit cell parameters and space groups of the various phases of the compound are determined following the standard procedure. According to the data on the initial phase symmetry reported in Section 2 (space group $Fm\bar{3}m$, $Z = 4$), Rb_2KTiOF_5 is isostructural to elpasolites Rb_2KCrF_6 and Rb_2KGaF_6 [18]. Because of this, the structure of the cubic phase was not searched and, in order to refine the atomic coordinates of the initial and distorted phases of the oxyfluoride, we used the data for fluorides

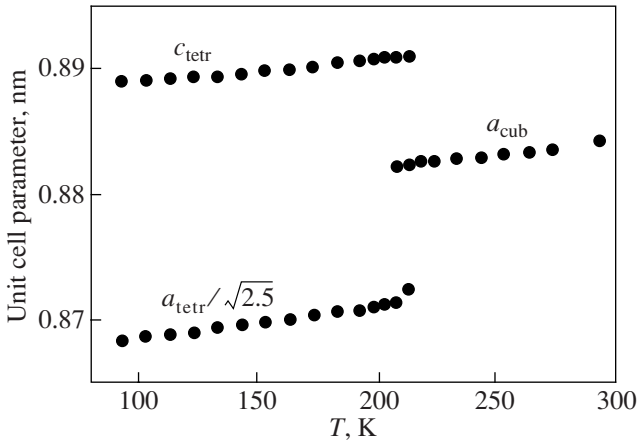

Fig. 7. Temperature dependence of the unit cell parameters of Rb_2KTiOF_5.

as the initial data. The refinement was performed using a full-profile method of minimizing the difference between the derivatives realized in the DDM program [19], which permits the correct subtraction of the background from the experimental x-ray diffraction pattern. Table 1 lists the main parameters of the data acquisition and of the structure refinement. The phase transition causes a tetragonal distortion (space group $I4/m$, $Z = 10$) accompanied by a significant increase in the unit cell volume; the relationships between the unit cell parameters of the phases are as follows: $a_{tetr} = (3a_{cub} - b_{cub})/2$, $b_{tetr} = (3b_{cub} + a_{cub})/2$, and $c_{tetr} = c_{cub}$.

An analysis of the cubic and low-temperature phases shows that the phase transition causes the rotation of all the octahedra around the fourth-order axis through an angle of ~3°. As a result of the phase transition, part of the $TiOF_5$ octahedra undergo distortions. We determined the positions of all ligands of these polyhedra; none of them is taken into another under symmetry operations. However, owing to the similarity of the F and O atomic scattering functions, we failed to identify the oxygen atom among the six ligands. The other polyhedra have the form of almost regular octahedra since they are arranged on the fourth-order symmetry axes; thus, we were not able to distinguish the sites of the four atoms in the plane perpendicular to such an axis. One of the most important results of the phase transition is the significant displacement of the Rb cations (~0.2 Å).

Table 1. Parameters of the data acquisition and refinement of the structure of the Rb_2KTiOF_5 compound at $T = 297$ and 100 K

Parameter	$T = 297$ K	$T = 100$ K
Space group	$Fm\bar{3}m$	$I4/m$
Number of formula units, Z	4	10
a, Å	8.8675(6)	13.814(1)
c, Å		8.887(1)
V, Å^3	697.27(9)	1695.8(4)
Angular range 2θ, deg	5.733–53.77	5.733–40
Number of Bragg reflections	114	866
Number of refined parameters	6	21
R_{DDM}, %	4.02	4.69
R_{wp}, %	8.04	9.38
R_B, %	3.90	4.72

Note: a and c are the unit cell parameters, and V is the unit cell volume. The reliability factors: R_{DDM} is the DDM factor [19], R_{wp} is the weight profile factor, and R_B is the Bragg factor.

The complex x-ray diffraction studies described in Sections 2 and 5 give the temperature dependence of the cubic and tetragonal unit cell parameters related by the relationships $a_{tetr} \approx a_{cub}\sqrt{2.5}$ and $c_{tetr} \approx a_{cub}$ over a wide temperature range (Fig. 7). We clearly see abrupt changes in the parameters at the transition temperature (indicating that the transformation is of first order) and their slight changes at $T < T_0$.

6. DISCUSSION OF THE RESULTS

As noted above, before the start of this study, there had been only data on the influence of the cation substitution on the phase transition temperature in titanium oxyfluorides (cryolites with atomic cations). However, the studies of fluorine–oxygen compounds with anions of other local symmetry (e.g., $MO_3F_3^{3-}$) have shown that the cubic phase of elpasolites is stabilized down to room temperature. In this case, structural distortions remain ferroelectric in character [16]. Based on these data and the data from [4], one could expect the behavior of the titanium analogs to be similar.

However, the experimental data obtained in our comprehensive studies of the oxyfluoride Rb_2KTiOF_5 are not all consistent and we cannot make unambiguous conclusions even concerning the number of phase transitions and their character.

We believe that our data on the anomalous behavior at 215 K of the heat capacity, unit cell parameters, permittivity, and DTA signal are most reliable and can be interpreted with confidence, and they allow the conclusion that the elpasolite Rb_2KTiOF_5 undergoes a structural phase transition below room temperature, as would be expected with the data from [4]. Despite the absence of a pronounced latent heat (jump in entropy), the transition is of first order and is accompanied by large thermal hysteresis δT_0 and a large jump in the unit cell parameters. This conclusion is also confirmed by a small stepwise change in the permittivity at T_0, which can, according to the thermodynamic theory of phase transitions [20], be interpreted as a change characteristic of first-order nonferroelectric structural transformations.

Knowing the dependences of the unit cell parameters and the pressure coefficient for Rb_2KTiOF_5, we can estimate the entropy jump δS_0 from the Clausius–Clapeyron equation $dT_0/dp = (\delta v_0/v)/\delta S_0$, where δv_0 is the volume jump at the transition point, which is equal, for tetragonal distortions, to the sum of the jumps in the lattice parameters $\delta c + 2\delta a$. The calculated value $\delta S_0 = 11.5$ J/mol K is fairly close to the value found from the $\Delta S(T)$ dependence (Fig. 5) in the temperature range $T_0 \pm 3$ K corresponding to the symmetric part of the anomalous peak in the heat capacity (Fig. 4c), which can be associated with spreading of the latent heat due, in particular, to the sample imperfection.

The possible existence of a second transition is supported by the following experimental facts: (1) the splitting of the (400) reflection into three peaks and its subsequent transformation into two peaks in some temperature range $T < T_0$ and (2) the existence of a very small shoulder in the heat capacity anomaly near 208–210 K. However, if the low-temperature phase transition occurred, then all the unit cell parameters would change abruptly at the first-order phase transition point and a $C_p(T)$ anomaly would be observed in the form of a sharp peak. In the case of a second-order phase transition in the 15-K-wide range below T_0, smooth variations in the parameters would be observed. The absence of a second-order transition is supported by the experimental time transformation of the (400) reflection at $T < T_0$ described in Section 2, which is more likely to indicate the coexistence of two phases (cubic and tetragonal) over a wide temperature range.

Let us return to the structural transformation at 215 K. Based on the thermodynamic parameters of cryolites $A_3MO_3F_3$ with atomic cations [1], we could expect, by analogy, a small change in the entropy corresponding to the structural distortion of Rb_2KTiOF_5. In actuality, this change is large ($\approx R\ln 8$), which is characteristic of order–disorder transitions. Note that we observed a close value of the entropy change in the related titanate $(NH_4)_3TiOF_5$ undergoing a pronounced first-order transition with a reliably determined latent heat [15]. The structure of the cubic phase of the latter oxyfluoride was assumed to be disordered owing to the presence in it of the NH_4 group in the 4*b* position. In this position, the tetrahedron must be orientationally disordered according to the symmetry of the surroundings, occupying at least two positions, which, in turn, can cause disordering of the anion sublattice. From analyzing the calorimetric and x-ray diffraction data, we conclude that the structural distortion in the titanium–ammonium cryolite is due to a complete or partial ordering of the tetrahedral and octahedral groups, respectively [15]. Based on the composition of the building blocks in Rb_2KTiOF_5, we can conclude that only the anion can be orientationally disordered in this compound. It should be noted, however, that the thermal factors of the F and O atoms in this compound are substantially smaller than those in the ammonium analog (Table 2) [21]. On the other hand, it is seen from Table 2 that the thermal parameter of the Rb atom is fairly large and is comparable to B_{iso} for F(O), which, in combination with the experimentally observed significant displacements of Rb atoms in the distorted phase (Section 5), allows us to assume a possible positional disordering of rubidium in the $Fm\bar{3}m$ phase in the [111] direction.

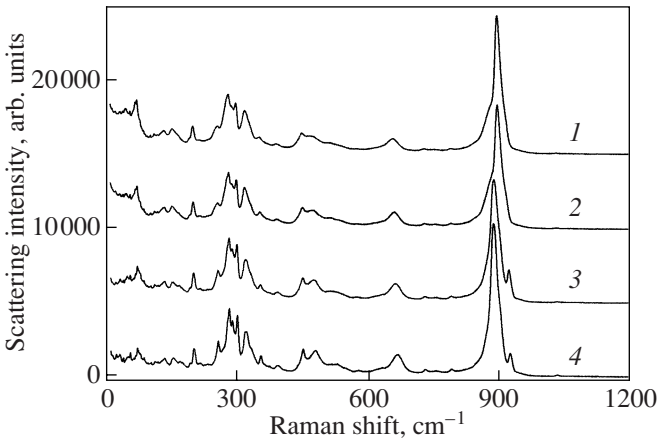

Fig. 8. Raman spectrum of Rb_2KTiOF_5 at temperatures of (*1*) 288, (*2*) 218, (*3*) 178, and (*4*) 78 K.

Information on the structural disordering of the primary and distorted phases can also be obtained from the Raman spectra measured in the frequency range 10–1200 cm^{-1} in the temperature range 77–300 K (Fig. 8). First, in the low-frequency spectral range of the high-temperature phase, the central peak has a shoulder, which is indicative of disordering of some building blocks; this disordering disappears after the phase transition. Second, the shape of the peak near 900 cm^{-1}

Table 2. Thermal parameters B_{iso} of atoms in various crystallographic positions of the cubic phase and the thermodynamic parameters of the phase transitions in Rb_2KTiOF_5, $(NH_4)TiOF_5$ [15, 21] and Rb_2KGaF_6 [18, 22]

Position	B_{iso}, Å^2		
	Rb_2KTiOF_5	$(NH_4)_3TiOF_5$	Rb_2KGaF_6
4*a*	2.6(2)	2.34(8)	0.96
4*b*	2.0(2)	4.7(4)	1.02
8*c*	3.57(7)	3.4(2)	2.08
24*e*	4.1	11.1	3.08
Parameter			
T_0, K	215	264.7	123.2
ΔT_0, K	6.1	2.3	6
ΔS_0, J/mol K	17.0	18.1	14.4
dT_0/dp, K/GPa	109.6	6.3	112

associated with the Ti–O vibrations suggests that the ligands in the $TiOF_5$ octahedra are disordered. All lines of this group are present in the spectra of both the cubic and tetragonal phases. However, as a result of the phase transition, the frequencies are changed significantly and fairly sharply. The large width of the central line of the distorted phase shows that the octahedral subsystem remains disordered. This fact agrees with the proposed model of the structure of the distorted phase in which the octahedra lying on the fourth-order axes of the $I4/m$ unit cell are likely to remain disordered.

The thermal hysteresis (about 6 K) in the temperature dependence of the parameters of the experimental Raman spectra is close to that found in the calorimetric measurements.

Thus, based on the calorimetric, structural, and spectroscopic studies, one can assume that the large entropy of the phase transition in Rb_2KTiOF_5 may be due to the following factors: the rotation of all octahedra around the fourth-order axis, complete ordering and distortion of some octahedra, and the significant displacement of the Rb atoms.

Rb_2KTiOF_5 is the only oxyfluoride with an elpasolite structure containing atomic univalent cations that has been studied in detail. It is interesting that the entropy, the hysteresis, and the shift in the temperature of the transition in this crystal under hydrostatic pressure are close to the respective characteristics of related fluorine elpasolites with the same composition of univalent cations, Rb_2KMF_6(M = Fe, Ga) (Table 2) [22, 23]. These crystals, as well as Rb_2KTiOF_5, do not exhibit the classical behavior of the heat capacity associated with the latent heat of a phase transition δH_0. Moreover, the heat capacity anomaly, e.g., for Rb_2KGaF_6, is a symmetric peak near $T_0 \pm 8.5$ K [23], which can be interpreted as being due to spreading δH_0. For comparison, Table 2 presents the thermal parameters of the atomic vibrations in the $Fm\bar{3}m$ phase of the fluoride calculated in the isotropic approximation. There is a correlation between these parameters and those of Rb_2KTiOF_5. Moreover, the displacements of the Rb atoms as a result of the phase transition are comparable in both elpasolites.

However, in the fluoride, as a result of the transition to the phase with the same symmetry ($I4/m$) as that of the oxyfluoride, the 1/5 octahedral GaF_6 groups are rotated through an anomalously large angle of 45° around the fourth-order axis [18]. In this case, the coordination of some potassium atoms is changed and the octahedral KF_6 groups are transformed into pentagonal bipyramids. Thus, despite the similarity of most characteristics of structural distortions, the mechanism of the phase transition $Fm\bar{3}m$ ($Z = 4$) $\rightleftarrows$ $I4/m$($Z = 10$) in Rb_2KTiOF_5 differs substantially from that proposed in [18] for the fluorine elpasolites.

7. CONCLUSIONS

In this work, we have performed for the first time detailed studies of the heat capacity, structure, permittivity, p–T phase diagram, and Raman spectra of one of the titanium oxyfluorides $A_2A'TiOF_5$ with atomic univalent cations exhibiting the elpasolite/cryolite structure.

It has been established that the elpasolite Rb_2KTiOF_5 undergoes at 215 K a structural first-order transition $Fm\bar{3}m$ ($Z = 4$) $\rightleftarrows$ $I4/m$($Z = 10$) accompanied by a significant jump in the unit cell volume ($\delta v/v \approx 1.2\%$). The studies of the structure and the Raman spectra of the cubic phase of Rb_2KTiOF_5 showed that disordering takes place at least in the octahedral subsystem, which correlates with the large entropy change ($\Delta S_0 \approx R\ln 8$).

The structural distortion is due to the rotation of all octahedra around the fourth-order axis through an angle of ~3°, a distortion of some octahedra, and the significant displacements of the Rb atoms occupying the 8c position. When refining the structure, we failed to identify the F and O atoms even in the distorted phase.

The $\varepsilon(T)$ dependence near the phase transition is characteristic of nonferroelectric structural transformations.

The results have been analyzed in combination with the data for related fluorides Rb_2KMF_6, which undergo a phase transition to the same tetragonal phase $I4/m$ ($Z = 10$) and are also characterized by anomalously large parameters δT_0, dT_0/dp, ΔS_0, and $\delta v_0/v$. It has been established that the composition of the six-coordinated anion has a substantial effect on the structural distortions of fluorides and oxyfluorides.

ACKNOWLEDGMENTS

This work was supported by the Russian Foundation for Basic Research, project no. 06-02-16102.

REFERENCES

1. G. Peraudeau, J. Ravez, P. Hagenmüller, and H. Arend, Solid State Commun. **27**, 591 (1978).
2. M. Couzi, V. Rodriguez, J. P. Chaminade, M. Fouad, and J. Ravez, Ferroelectrics **80**, 109 (1988).
3. V. D. Fokina, I. N. Flerov, M. V. Gorev, M. S. Molokeev, A. D. Vasiliev, and N. M. Laptahs, Ferroelectrics **347**, 60 (2007).
4. G. Pausewang and W. Rüdorff, Z. Anorg. Allg. Chem. **364**, 69 (1969).
5. K. Dehnicke, G. Pausewang, and W. Rüdorff, Z. Anorg. Allg. Chem. **366**, 64 (1969).
6. M. Fouad, J. P. Chaminade, J. Ravez, and P. Hagenmüller, Rev. Chim. Miner. **24**, 1 (1987).
7. M. Hamadene, J. Grannec, J. Ravez, and A. Laœdoudi-Guehria, J. Fluorine Chem. **78**, 141 (1996).

8. F. J. Brink, L. Noren, D. J. Goossens, R. L. Withers, Y. Liu, and C.-N. Xu, J. Solid State Chem. **174**, 450 (2003).
9. F. J. Brink, R. L. Withers, K. Friese, G. Madariaga, and L. Noren, J. Solid State Chem. **163**, 267 (2002).
10. F. J. Brink, L. Noren, and R. L. Withers, J. Solid State Chem. **174**, 44 (2003).
11. I. N. Flerov, M. V. Gorev, V. D. Fokina, A. F. Bovina, M. S. Molokeev, E. I. Pogorel'tsev, and N. M. Laptash, Fiz. Tverd. Tela (St. Petersburg) **49** (1), 136 (2007) [Phys. Solid State **49** (1), 141 (2007)].
12. I. N. Flerov, V. D. Fokina, A. F. Bovina, E. V. Bogdanov, M. S. Molokeev, A. G. Kocharova, E. I. Pogorel'tsev, and N. M. Laptash, Fiz. Tverd. Tela (St. Petersburg) **50** (3), 497 (2008) [Phys. Solid State **50** (3), 515 (2008)].
13. I. N. Flerov, M. V. Gorev, V. D. Fokina, A. F. Bovina, M. S. Molokeev, Yu. V. Boĭko, V. N. Voronov, and A. G. Kocharova, Fiz. Tverd. Tela (St. Petersburg) **48** (1), 99 (2006) [Phys. Solid State **48** (1), 106 (2006)].
14. M. S. Molokeev, A. D. Vasiliev, and A. G. Kocharova, Powder Diffr. **22**, 227 (2007).
15. I. N. Flerov, M. V. Gorev, V. D. Fokina, A. F. Bovina, and N. M. Laptash, Fiz. Tverd. Tela (St. Petersburg) **46** (5), 888 (2004) [Phys. Solid State **46** (5), 915 (2004)].
16. G. Peraudeau, J. Ravez, and H. Arend, Solid State Commun. **27**, 515 (1978).
17. I. N. Flerov, K. S. Aleksandrov, V. G. Khlyustov, and N. V. Beznosikova, Fiz. Tverd. Tela (Leningrad) **14** (11), 3374 (1972) [Sov. Phys. Solid State **14** (11), 2853 (1972)].
18. F. J. Zuniga, A. Tressaud, and J. Darriet, J. Solid State Chem. **179**, 3607 (2006).
19. L. A. Solovyov, J. Appl. Crystallogr. **37**, 1 (2004).
20. B. A. Strukov and A. P. Levanyuk, *Ferroelectric Phenomena in Crystals: Physical Foundations* (Nauka, Moscow, 1983; Springer, Berlin, 1998).
21. I. N. Flerov, M. V. Gorev, V. D. Fokina, M. S. Molokeev, A. D. Vasil'ev, A. F. Bovina, and N. M. Laptash, Fiz. Tverd. Tela (St. Petersburg) **48** (8), 1473 (2006) [Phys. Solid State **48** (8), 1559 (2006)].
22. M. V. Gorev, I. N. Flerov, V. N. Voronov, A. Tressaud, J. Grannec, and J.-P. Chaminade, Fiz. Tverd. Tela (St. Petersburg) **36** (4), 1121 (1994) [Phys. Solid State **36** (4), 609 (1994)].
23. M. V. Gorev, I. N. Flerov, A. Tressaud, and J. Grannec, Fiz. Tverd. Tela (St. Petersburg) **39** (10), 1844 (1997) [Phys. Solid State **39** (10), 1647 (1997)].

Translated by Yu. Ryzhkov